Axial Ligation and Stoichiometry of Heme Centers in Adrenal Cytochrome b_{561}[†]

Yury Kamensky,*[,‡] Wen Liu,[§] Ah-Lim Tsai,[§] Richard J. Kulmacz,[§] and Graham Palmer*[,‡]

Department of Biochemistry and Cell Biology, Rice University, Houston, Texas 77251, and Department of Internal Medicine, University of Texas Health Science Center at Houston, Houston, Texas 77030

Received January 11, 2007; Revised Manuscript Received May 20, 2007

ABSTRACT: Cytochrome (cyt) b_{561} transports electrons across the membrane of chromaffin granules (CG) present in the adrenal medulla, supporting the biosynthesis of norepinephrine in the CG matrix. We have conducted a detailed characterization of cyt b_{561} using electron paramagnetic resonance (EPR) and optical spectroscopy on the wild-type and mutant forms of the cytochrome expressed in insect cells. The $g_z = 3.7$ (low-potential heme) and $g_z = 3.1$ (high-potential heme) signals were found to represent the only two authentic hemes of cyt b_{561}; models that propose smaller or greater amounts of heme can be ruled out. We identified the axial ligands to hemes in cyt b_{561} by mutating four conserved histidines (His54 and His122 at the matrix-side heme center and His88 and His161 at the cytoplasmic-side heme center), thus confirming earlier structural models. Single mutations of any of these histidines produced a constellation of spectroscopic changes that involve not one but both heme centers. We hypothesize that the two hemes and their axial ligands in cyt b_{561} are integral parts of a structural unit that we term the "kernel". Histidine to glutamine substitutions in the cytoplasmic-side heme center but not in the matrix-side heme center led to the retention of a small fraction of the low-potential heme with $g_z = 3.7$. We provisionally assign the low-potential heme to the matrix side of the membrane; this arrangement suggests that the membrane potential modulates electron transport across the CG membrane.

Most, if not all, eukaryotic organisms carry a gene for at least one member of the newly discovered protein family of cytochrome b_{561} (cyt b_{561})[1] (*1*−*4*). The first known member of the family, adrenal-type cyt b_{561}, is essentially an ascorbate-regeneration machine (*5*) that plays a key role in supplying electrons for the biosynthesis of norepinephrine by dopamine-β-hydroxylase (*6*) and of several important peptide hormones by peptidylglycine α-monooxygenase (*6*). Several other cyt b_{561} family members are either suggested to participate in ascorbate metabolism or to depend upon ascorbate for ferric-reductase activity. Among them are stromal-cell-derived receptor 2, which is an iron reductase expressed in major iron-storage organs (*7*, *8*); a newly discovered analogue with ferric-reductase activity, Lcyt b_{561}, which was found in macrophage lysosomes (*9*); Tcyt b_{561}, a cytochrome recently reported as a constituent of the tonoplast membrane in *Arabidopsis* (*10*); mammalian duodenal b_{561} (Dcyt b_{561}), which participates in the uptake of dietary iron in the brush border membrane of the duodenum (*8*, *11*) (but see refs *12* and *13*) and the iron uptake in airway epithelial cells (*14*) and possibly plays a role in extracellular ascorbate recycling in human erythrocytes (*15*). Another interesting member of the cyt b_{561} family is the 101F6 protein, a putative tumor suppressor with an unknown mechanism of action (*16*, *17*). Many species have multiple cyt b_{561} family members, with 6 known in humans and as many as 16 in *Arabidopsis thaliana*. Thus, the cyt b_{561} family appears to be important for the biology of eukaryotes (*1*).

With most of the proteins constituting this family still waiting for physicochemical characterization, the development of a structural and functional model of a prototypic representative would be valuable as a point of comparison. Adrenal cyt b_{561} is undoubtedly the current best choice for such a prototype because (a) a significant database already exists for this protein, (b) it is highly abundant, comprising 17% of the total protein in its natural source, the membrane of chromaffin granules (CG) located in the medulla of adrenal glands (*18*), and (c) it has been expressed in fully functional form in insect (*19*, *20*), yeast (*20*, *21*), and recently bacterial (*22*) cells.

According to the current paradigm (*5*), the synthesis of each molecule of norepinephrine by dopamine-β-hydroxylase within CG requires two electrons provided by intragranular ascorbic acid (*6*). In this process, two ascorbic acid molecules inside the granule undergo one-electron oxidation to monodehydroascorbate (*23*) and must be replenished. Neither fully reduced ascorbate nor matrix monodehydroascorbate can penetrate the granule membrane (*24*−*26*), and cyt b_{561} regenerates intragranular ascorbate by

[†] This work was supported by American Heart Association (Texas Affiliate) Grant 0455107Y (to G.P.) and National Institutes of Health Grant GM44911 (to A.-L.T.).

* To whom correspondence should be addressed: Department of Biochemistry and Cell Biology, Rice University, Houston, TX 77251. Telephone: 713-348-3903. Fax: 713-348-5154. E-mail: yuryk@bioc.rice.edu (Y.K.); Department of Biochemistry and Cell Biology, Rice University, Houston, TX 77251. Telephone: 713-348-4860. Fax: 713-348-5154. E-mail: graham@bioc.rice.edu (G.P.).

[‡] Rice University.

[§] University of Texas Health Science Center at Houston.

[1] Abbreviations: cyt, cytochrome; CG, chromaffin granules; M, matrix; C, cytoplasmic; MDA, monodehydroascorbate; PAL, putative axial ligand; EPR, electron paramagnetic resonance; HALS, highly axial low spin; ALA, δ-aminolevulinic acid; EDTA, ethylenediamine tetraacetic acid; DM, *n*-dodecyl-β-D-maltoside; CHAPS, 3-[(3-cholamidopropyl)dimethylamino]-1-propanesulfonate; SVD, singular value decomposition.

10.1021/bi700054g CCC: $37.00
Published on Web 06/30/2007

transferring electrons acquired from cytoplasmic ascorbate (*5*, *27*−*32*).

Adrenal cyt b_{561} consists of 252 amino acid residues with a M_r of 28 kDa (*33*, *34*). Sequence analysis of adrenal cyt b_{561} predicts six transmembrane helices (*33*), with the central four helices forming a bundle (*3*) carrying the hemes (*35*). Although all models of cyt b_{561} beginning with that of Degli Esposti et al. (*35*) consider cyt b_{561} to contain two hemes, the heme stoichiometry has remained an unsettled issue. On the basis of an apparent heme/protein ratio of 1, early literature considered cyt b_{561} to contain a single heme (*27*, *36*−*39*). Tsubaki et al. (*40*) developed a mild purification procedure and reported the isolation from CG of cyt b_{561} containing two hemes. Subsequent expression and purification of a recombinant, His-tagged bovine cyt b_{561} from yeast, bacterial, and insect cells also yielded proteins with two hemes per polypeptide (*20*, *22*). The two hemes were reported to have different low-spin signals in electron paramagnetic resonance (EPR) spectra, with low-field g values of 3.1 and 3.7 (*40*−*42*), although recently Wanduragala et al. (*43*) raised doubts regarding the authenticity of the $g_z = 3.7$ signal in their sample of purified cyt b_{561}. Kipp et al. (*44*) suggested that the second EPR signal is not a manifestation of an independent heme center but represents the heme−heme interaction between two different monoheme protein molecules. On the other hand, Burbaev et al. (*41*) and later Kamensky et al. (*19*) observed heterogeneity in the EPR signal of one of the hemes and noted the possibility that membranous cyt b_{561} contained three hemes (*41*), perhaps in the framework of a dimeric structure (*19*).

Bis-histidine ligation is very likely for all of the hemes of cyt b_{561} (*41*, *45*). Kamensky et al. (*45*) observed that cyt b_{561} lacks the characteristic charge-transfer band near 700 nm that is typical for methionine coordination in cytochromes *c* (*46*) and in cyt b_{562} from *Escherichia coli* (*47*). In addition, the marked similarity of the magnetic circular dichroism in the β-band of reduced cyt b_{561} with that of cyt b_5 (*45*) and the bis-imidazole complex of protoheme makes coordination by lysine unlikely (*48*), leaving the imidazole side chain of histidines as the most credible candidates for axial ligands to heme in cyt b_{561} (*45*). The EPR spectral characteristics of cyt b_{561} (*20*, *21*, *40*−*42*) are consistent with histidine axial ligands, as are the near-infrared magnetic circular dichroism spectra of cyt b_{561} (Duin, E., Kamensky, Y., Johnson, M., and Palmer, G., unpublished results).

Six fully conserved histidines (His54, His88, His92, His110, His122, and His161 in adrenal cyt b_{561}) have been identified in adrenal cyt b_{561} from different species (*1*). Degli Esposti et al. (*35*) and later other investigators (*1*−*3*, *49*) suggested that His54 and His122 are the axial ligands to the heme on the matrix (M) side of the CG membrane and that His88 and His161 provide axial ligation to the heme on the cytoplasmic (C) side. However, this hypothesis has been waiting for experimental confirmation. An important step in this direction was recently taken by Bérczi et al. (*21*). Their results suggested that His110 could be excluded from the list of potential axial ligands to heme and were consistent with the idea of His54, His88, His122, and His161 being the axial ligands. In the absence of an X-ray structure, the assignment of individual axial ligands to a particular heme center can be examined by EPR analysis of recombinant cyt b_{561} in which putative axial ligands (PALs) are replaced systematically by mutagenesis. EPR is very sensitive to the properties and environment of the oxidized (paramagnetic) heme centers of cytochromes (*50*), and importantly, the two heme EPR signals in cyt b_{561} are well resolved (*40*−*42*).

We present here a comparative EPR and optical study of natural and recombinant wild-type bovine adrenal cyt b_{561}, as well as its mutants, with the goal of resolving remaining questions regarding the fundamental characterization of cyt b_{561}, namely, the quantity of its hemes and identification of their axial ligands.

EXPERIMENTAL PROCEDURES

Materials. Hemin, dithiothreitol, EDTA, cholate, desoxycholate, ALA, and horse heart cytochrome *c* were from Sigma (St. Louis, MO). Frozen bovine adrenal glands were purchased from Pel-Freez (Rogers, AR), while fresh glands were obtained from a slaughterhouse. Protease inhibitor cocktail Set 1 and Set III (without EDTA) were from Calbiochem (San Diego, CA). Ascorbic acid sodium salt and sodium dithionite were obtained from Fluka (Germany). *n*-Octyl-β-D-glucoside and DM, CHAPS, PMAL-c12, and Triton X-100 were from Anatrace (Maumee, OH).

CG and CG Membrane Vesicles Preparation. Fresh and prefrozen adrenal glands were used for the preparation of CG and different types of membrane vesicles as described previously (*20*, *42*).

Cyt b_{561} from CG. Purification of cyt b_{561} from natural membranes was performed according to the protocol developed by Tsubaki et al. (*40*).

Recombinant Bovine Cyt b_{561}. Expression of His-tagged bovine cyt b_{561} in *Sf9* insect cells and purification of membranous and isolated recombinant protein were performed as described previously (*20*). The membranous preparations of mutated cyt b_{561} were prepared by the method developed in ref *20* for the wild type, where the membranes were collected at 150,000*g* with or without prior removal of the 500*g* and 15,000*g* fractions. Site-directed mutagenesis of bovine cyt b_{561} was performed on the b561/pBluescript II KS (+) plasmid using the QuikChange site-directed mutagenesis kit (Stratagene). The primer sequences containing the mutation (the bases changed are underlined) were His54Gln sense (5′-GCAGTTCAACGTGCAACCCCTCT-GCATGATCATAG-3′) and His54Gln antisense (5′-CTAT-GATCATGCAGAGGGGTTGCACGTTGAACTGC-3′), His54Met sense (5′-CTGCAGTTCAACGTGATGCCCCTCTGCAT-GATC-3′) and His54Met antisense (5′-GATCATGCA-GAGGGGCATCACGTTGAACTGCAG-3′), His54Tyr sense (5′-CTGCAGTTCAACGTGTACCCCCTCTGCATGATC-3′) and His54Tyr antisense (5′-GATCATGCAGAGGGGG-TACACGTTGAACTGCAG-3′), His88Gln sense (5′-ACCAAAGTCCTGCAAGGGCTGCTGCACGTCTTC-3′) and His88Gln antisense (5′-GAAGACGTGCAGCAGC-CCTTGCAGGACTTTGGT-3′), His122Gln sense (5′-AC-CTGTACAGCCTGCAAAGCTGGTGCGGCATCC-3′) and His122Gln antisense (5′-GGATGCCGCACCAGCTTTG-CAGGCTGTACAGGT-3′), His161Gln sense (5′-GCTAC-CGCCCGCAGCAAGTCTTCTTCGGCG-3′) and His161Gln antisense (5′-CGCCGAAGAAGACTTGCTGCGGGCGG-TAGC-3′), His161Met sense (5′-CGCTACCGCCCGCA-GATGGTCTTCTTCCGGCGC-3′) and His161Met antisense (5′-GCGCCGAAGAAGACCATCTGCGGGCGGTAGCG-

3′), and His161Tyr sense (5′-CGCTACCGCCCGCAG-TACGTCTTCTTCGGCG-3′) and His161Tyr antisense (5′-CGCCGAAGAAGACGTACTGCGGGCGGTAGCG-3′).

E. coli strain XL-10 (Stratagene) competent cells were heat-transformed with the mutagenesis reaction, plated on LB agar containing 100 μg/mL ampicillin, and grown overnight. Ampicillin-resistant colonies were grown in LB−ampicillin broth at 37 °C overnight, and plasmid DNA was isolated. Clones were screened for the presence of the desired mutation by DNA sequencing, digested with *Bam*HI/*Xba*I, and separated on an agarose gel. The purified DNA fragments containing the desired mutations were inserted into *Bam*HI/*Xba*I-digested pVL1393 vector (PharMingen, San Diego, CA). The final constructs were verified by restriction enzyme digestion and DNA sequencing. Construction of baculoviral vectors for the expression of mutant cyt b_{561} in insect cells followed published procedures (*51*).

Assay of Protein, Cyt b_{561}, and Heme Content. Total protein was assayed with a BioRad DC kit, using bovine serum albumin as the standard. Recombinant cyt b_{561} content was calculated using a difference extinction coefficient of 34 mM^{-1} cm^{-1} [561−575 nm, reduced minus oxidized spectrum (*20*)]. The concentration of membranous and purified CG cyt b_{561} was calculated using a difference extinction coefficient 37.3 mM^{-1} cm^{-1} [561−575 nm, reduced minus oxidized spectrum (*40*)]. The heme content was determined by the pyridine hemochrome assay (*52*), using a difference extinction coefficient (556−538 nm) of 24.5 mM^{-1} cm^{-1} (*53*).

EPR Sample Preparation. Samples were oxidized with an excess of ferricyanide. Membranous samples were then washed twice by centrifugation (1 h at 120,000*g*) to remove the oxidant, whereas detergent extracts and purified cytochrome were desalted using 10DG columns (BioRad). Concentrated samples were supplemented with 18% glycerol (50% glycerol for CG samples), transferred into EPR tubes, frozen in ∼1 s in a dry ice/ethanol mixture, and stored in liquid nitrogen. Typical cyt b_{561} monomer concentrations were 25−40 μM for membranous preparations and 50−70 μM of protein for isolated cytochrome.

Spectroscopy. Electronic absorption spectra were recorded with a Shimadzu Model 2101PC or a Jasco Model V-560 spectrophotometer at room temperature. EPR spectra were collected at 5−40 K with a Bruker EMX or a Varian E-6 spectrometer equipped with a liquid helium cryostat.

Computer Analysis. Experimental data were analyzed using fitting routines [including the SVD algorithm] of IgorPro 5.04 (Wavemetrics, Portland, OR). Molecular graphics of the cyt b_{561} structural model (*3*) were prepared using the software Ribbons 3.22 (*54*).

RESULTS

Stoichiometry and EPR Signals of the Hemes in Cyt b_{561}. Cyt b_{561} displays two distinct low-spin ferric heme signals, with g_z at 3.7 and 3.1 (Figure 1). We found the same two low-spin signals in all samples of cyt b_{561} examined: in intact CG, which is a preparation intermediate between the parent chromaffin cells and purified membrane (trace 1 in Figure 1); in purified CG membranes (traces 2 and 3 in Figure 1); and in purified wild-type, His-tagged cyt b_{561} expressed in insect cells (trace 4 in Figure 1).

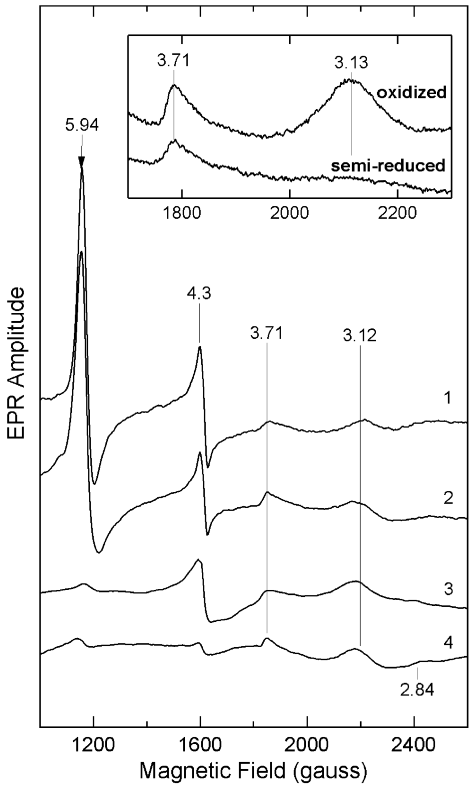

FIGURE 1: EPR signals of cyt b_{561} hemes in native CG, CG membranes, and the purified cytochrome. EPR spectra were recorded for freshly prepared CG (trace 1), "Tsubaki membranes" (as defined in ref *20*) (trace 2), "traditionally prepared" (*20*) CG membranes (trace 3), and purified His-tagged cyt b_{561} expressed in *Sf*9 cells (trace 4). Signal amplitudes were normalized to the heme concentration. Membranous samples (traces 1−3) were suspended in 20 mM Tris at pH 7.2 with 18% glycerol, except for freshly prepared CG, where the glycerol concentration was 50%. The purified cytochrome sample (trace 4) was in 100 mM sodium phosphate at pH 7.2 containing 18% glycerol and 1% octyl glucoside. The microwave power and temperatures were: 1, 15 mW and 11 K; 2, 32 mW and 11 K; 3, 50 mW and 11 K; and 4, 15 mW and 8 K. Other spectrometer settings were: microwave frequency, 9.60 GHz; modulation frequency, 100 kHz; and modulation amplitude, 10 G, except for trace 3 (20 G). (Inset) EPR signals for oxidized and semireduced cyt b_{561} hemes in CG membranes. "Traditionally prepared" CG membranes were suspended in 50 mM Hepes at pH 7.2 with 0.1 mM EDTA and 18% glycerol and either oxidized with ferricyanide (upper) or 50% reduced with ascorbate (lower) before spectra were recorded at 11.5 K with a microwave power of 50 mW. Other spectrometer settings were: microwave frequency, 9.27 GHz; modulation frequency, 100 kHz; and modulation amplitude, 20 G.

In addition to the g_z ∼3.7 and 3.1 signals, there is a signal from non-heme iron at $g = 4.3$ that is prominent in membranous samples (traces 1−3 in Figure 1) but rather insignificant in the sample of purified cytochrome (trace 4 in Figure 1). The small size of the signal at $g \sim 6$ establishes that only a very small fraction of the purified cytochrome is in the high-spin form (trace 4 in Figure 1). CG membranes prepared according to a traditional protocol (*42*) also exhibit a low level of high-spin species (trace 3 in Figure 1). Intact CG and Tsubaki membranes (*20*) have a somewhat higher content of the high-spin signal (traces 1 and 2 in Figure 1). The small signal at $g_z = 2.84$, which is present in some of our experiments (e.g., trace 4 in Figure 1), was previously shown to derive reversibly from the $g_z = 3.1$ signal in a

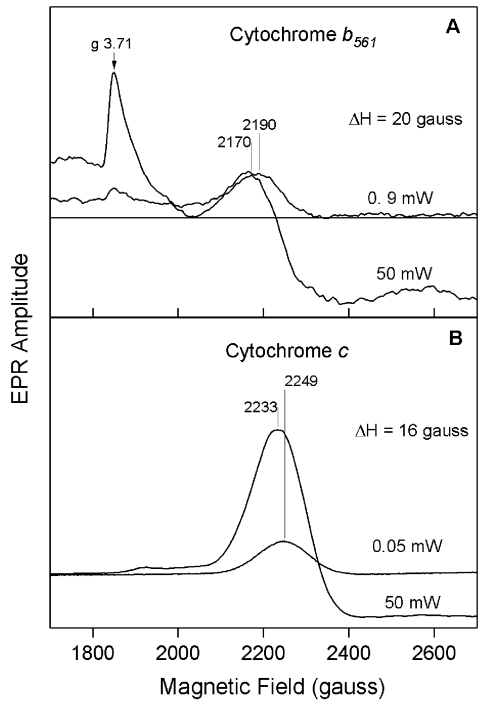

FIGURE 2: Effects of the microwave power on the EPR signal of the high-potential heme of cyt b_{561}. (A) EPR spectrum of 31 μM purified cyt b_{561} from CG membranes in 50 mM sodium phosphate at pH 7.3 containing 18% glycerol and 1% octyl glucoside recorded at 0.9 and 50 mW. (B) EPR spectrum of 200 μM horse heart cytochrome *c* in 60 mM sodium phosphate at pH 6.8 containing 20% glycerol recorded at 0.05 and 128 mW. Spectrometer conditions: microwave frequency, 9.60 GHz; modulation frequency, 100 kHz; modulation amplitude, 10 G; and temperature, 8.0 K.

pH-dependent manner, possibly reflecting deprotonation of an axial histidine (*40*).

The $g_z = 3.7$ and 3.1 signals have been assigned to the low- and high-potential heme centers, respectively, based on the order in which they were reduced in titrations with ascorbate (*40*, *41*). The inset of Figure 1 compares EPR spectra of fully oxidized and semireduced CG membranes. It is important to note that the location of the EPR signal of the low-potential heme remains unchanged, while its amplitudes diminish slightly; at the same time, the amplitude of the high-potential heme approaches zero, and no additional signals appears. This rules out a heme−heme electronic interaction in cyt b_{561} (see the Discussion).

Lowering the temperature of cyt b_{561} from 45 to 10 K was observed to shift the position of the high-potential peak from $g = 3.11$ to 3.14 without changing the position of the low-potential heme signal (*41*). The new heme's signal was hypothesized to have slightly different *g* values and significantly different relaxation properties (*41*). However, we suggest that the shift in the peak position represents a "passage artifact"[2] (*55*). This phenomenon is illustrated in Figure 2, which compares the effects of microwave power on the high-potential heme of cyt b_{561} (Figure 2A) and on cytochrome *c*, an undoubtedly homogeneous species at pH 7 (Figure 2B). In both proteins, increasing the microwave power shifted the position of the peak to lower fields and caused a baseline "overshoot" at higher fields. Passage artifacts may be encountered with any low-spin hemeprotein when the spin-lattice relaxation process is overwhelmed, as occurs at high powers or very low temperatures, and is not evidence for the presence of multiple heme centers in cyt b_{561}, as was originally suggested (*41*).

Global Analysis of Cyt b_{561} Absorption Spectra. We previously demonstrated that the high- and low-potential heme centers of cyt b_{561} in CG membranes have unique spectral features (*42*). In the current experiments, we utilized purified bovine adrenal cyt b_{561} expressed in yeast (*20*), thus improving the quality of the spectra by reducing the noise caused by light scattering and by eliminating optical interference from a minor component present in the CG membranes, a separate heme-containing protein with a low redox potential.[3] Figure 3A presents absolute absorption spectra of cyt b_{561} recorded during titration with ascorbate. Because the midpoint potentials of the two hemes differ by ~100 mV (*36*, *56*), spectral changes during the earlier stages of reduction reflect the reduction of the high-potential heme exclusively. This heme has a "split" α-band, with a pronounced maximum and a shoulder at a shorter wavelength (Figure 3B). As the titration progresses, the low-potential heme begins to contribute to the total absorbance and the spectra become somewhat more symmetric (Figure 3A) because the α-band of the low-potential heme is not split and consequently has a much smaller contribution at shorter wavelengths (Figure 3B).

To determine the number of spectral species necessary to explain all features of the absorption spectra at all stages of reduction, we subjected the set of 15 spectra shown in Figure 3A to SVD analysis. Figure 4A shows the relative amplitudes of the principal components derived from this analysis. It is clear that only SVD components 1 and 2 have significant amplitude and that the other components can be ignored. Note that the two major SVD components (Figure 4B) are not identical to either the spectrum of the cytochrome itself or the spectrum of either heme center shown in Figure 3B. However, using only these two components, the SVD decomposition can be reversed to reconstruct the important features of the spectra shown in Figure 3A. This is illustrated in Figure 4C, which shows experimental and calculated spectra at approximately 7, 50, and 100% reduction (corresponding to traces 1, 7, and 15 of Figure 3A). The major features of the experimental data are reproduced so closely that the discrepancies between ex-

[2] Passage artifacts arise when the rate of change of the total magnetic field incident on the sample is greater than the inverse of the spin-lattice relaxation time. Under these conditions, the EPR signal has contributions from both absorption and dispersion modes, and distortions in the EPR spectrum result [Mailer, C., and Taylor, C. P. (1973) Rapid adiabatic passage EPR of ferricytochrome *c*: Signal enhancement and determination of the spin-lattice relaxation time, *Biochim. Biophys. Acta 322*, 195−203].

[3] Our earlier publication [Kamensky, Y. A., and Palmer, G. (2001) Chromaffin granule membranes contain at least three heme centers, *FEBS Lett. 491*, 119−122] considered a third heme as either a cyt b_{561} component or another heme-containing protein present in the CG membrane. The fact that this third heme is not a part of cyt b_{561} itself is now confirmed, because neither purified cyt b_{561} from CG nor those expressed in insect, yeast, or bacterial cells contains a heme with a *g* factor of 3.62 that is not reduced by ascorbate. The origin and function of the third heme in CG remain unresolved, although Ponting speculated that it may be the heme of a cyt *b*-type iron reductase [Ponting, C. P. (2001) Domain homologues of dopamine β-hydroxylase and ferric reductase: Roles for iron metabolism in neurodegenerative disorders? *Hum. Mol. Genet. 10*, 1853−1858].

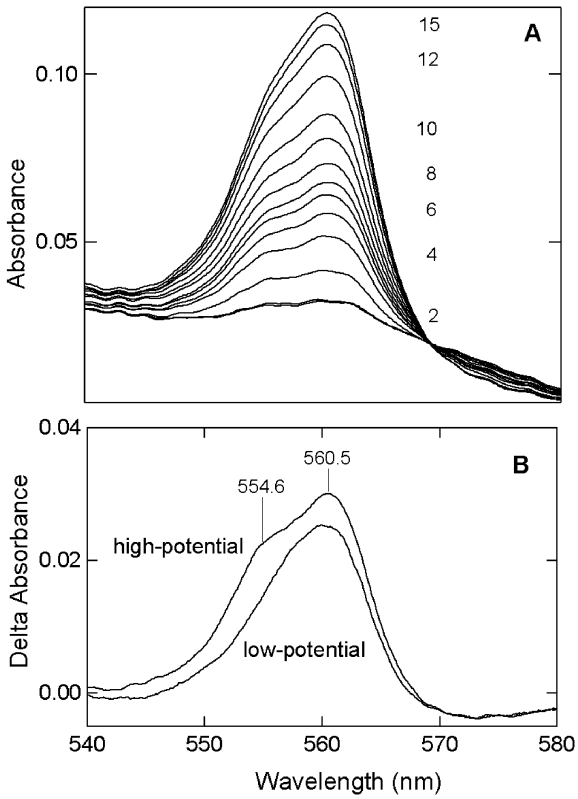

FIGURE 3: Absorption spectra of the high- and low-potential hemes of cyt b_{561}. (A) Absolute spectra of cyt b_{561} recorded during reductive titration with ascorbate. The purified cytochrome expressed in yeast (*20*) was diluted to 2.6 μM in 100 mM potassium phosphate at pH 7.2 containing 10% glycerol and 0.08% DM. Spectra were recorded after the addition of the following concentrations of ascorbate: 1, 0.3 μM; 2, 1.2 μM; 3, 5.2 μM; 4, 12.3 μM; 5, 22.4 μM; 6, 35.5 μM; 7, 52 μM; 8, 71 μM; 9, 105 μM; 10, 170 μM; 11, 0.53 mM; 12, 1.2 mM; 13, 8.5 mM; and 14 (not shown for clarity), 19.6 mM. Trace 15 was recorded after the addition of a few crystals of dithionite. Spectra were collected at 0.1 nm intervals with a 1.0 nm bandwidth and a scanning speed of 20 nm/min. (B) Difference spectra of individual heme centers calculated from spectra in A. High-potential heme, trace 6 minus trace 2; low-potential heme, trace 12 minus trace 9. Note that the spectra in 3B represent the shapes of the two components and not their relative amplitudes.

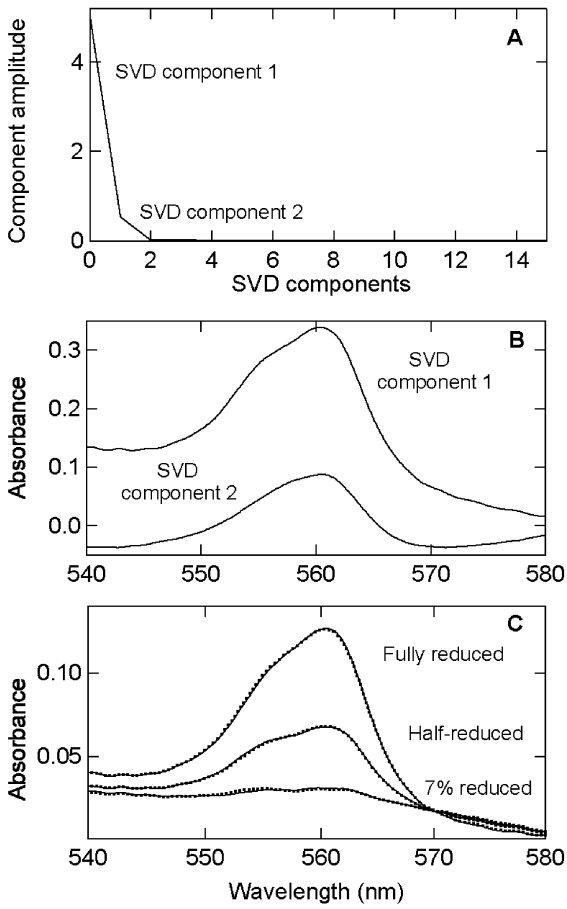

FIGURE 4: SVD analysis of absorption spectra of wild-type cyt b_{561} during reductive titration with ascorbate. (A) Relative amplitudes of the principal components derived from SVD analysis of the spectra shown in Figure 3A. (B) Spectra of the two major components in A. (C) Reconstruction of the 7% reduced, half-reduced, and fully reduced spectra from Figure 3A (traces 1, 7, and 15, respectively). The solid lines represent the original experimental data, and the dashed lines represent the reconstructed spectra using only principal components 1 and 2 from B.

perimental and synthetic curves are difficult to detect (Figure 4C). It is important to emphasize that just two SVD components are sufficient to reproduce all essential features of the cyt b_{561} absorption spectra, and hence, only two spectral species contribute to the data of Figure 3A.

Expression of PAL Mutant Cytochromes in Insect Cells. We used our established insect cell system (*20*) to express recombinant adrenal cyt b_{561} with mutations in individual PAL residues (histidines 54, 88, 122, and 161) for EPR analysis. The insect cell expression system produced the four PAL mutants in comparable amounts, as assessed spectrophotometrically (Figure 5). However, whereas more than 90% of the wild-type cyt b_{561} was extracted by detergent from insect cell membranes (*20*), less than 15% of the PAL mutant cytochromes were solubilized by detergent. DM (with or without PMAL-c12), octyl glucoside, Triton X-100, CHAPS, cholate, and deoxycholate were tried at a variety of detergent/protein ratios, without and with up to 8 M urea. Such detergent resistance is not unique to the insect cell system or to cyt b_{561}. PAL mutants of cyt b_{561} expressed in yeast also could not be solubilized with dodecyl maltoside (Liu, W., and Cao, D., unpublished results). Similar effects of PAL mutations on the extractability of the mutated protein were observed in a study of the heme *b* subunit of succinate: quinone reductase from *Bacillus subtilis* (*57*). As the PAL mutants of cyt b_{561} resisted solubilization, we proceeded with their characterization in the membrane fraction.

Absorption Spectra of Membranous PAL Mutant Cytochromes. Figure 5A presents the reduced minus oxidized difference absorption spectrum of wild-type cyt b_{561} expressed in insect cell membranes. The spectrum is typical for low-spin heme *b*-containing cytochromes, with pronounced α-, β-, and γ-bands; its characteristics are quite similar to those of the CG cytochrome (*40*, *42*), as well as the recombinant protein expressed in yeast (*20*, *21*). Panels B and C of Figure 5 present the absorption spectra of PAL mutants with individual histidines substituted by glutamine, methionine, or tyrosine. In addition to low-spin heme features, the spectrum of each of the mutants exhibits some high-spin characteristics (maxima at ~440−450, 480, and 624 nm), indicating that the mutations perturbed the spin state of the heme center(s).

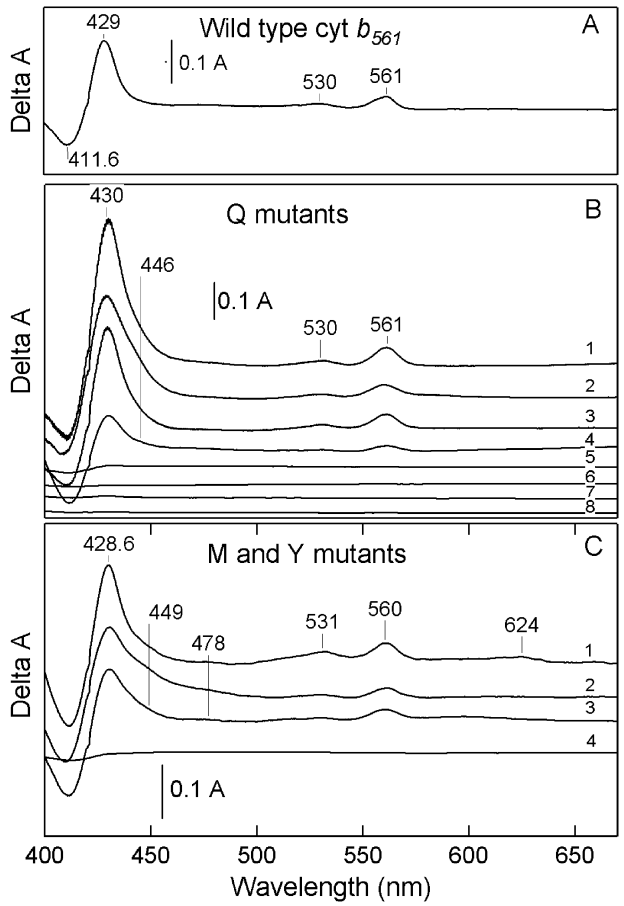

FIGURE 5: Reduced minus oxidized difference absorption spectra of wild-type and mutant cyt b_{561} in *Sf9* cell membranes. (A) Wild-type cyt b_{561}. (B) 1, H161Q; 2, H122Q; 3, H88Q; 4, H54Q; 5, membranes from cells expressing XylE or supplemented with ALA and hemin; 6, membranes from unsupplemented cells expressing XylE; 7, membranes from uninfected cells supplemented with ALA and hemin; and 8, membranes from unsupplemented, uninfected cells. (C) 1, H161Y; 2, H161M; 3, H54Y; and 4, membranes from cells expressing XylE and supplemented with ALA and hemin. All membrane samples were suspended in 60 mM Tris at pH 7.4 containing 20% glycerol and were reduced with a few grains of dithionite. The absolute absorption spectra were collected at 0.2 nm intervals with a 0.1 nm bandwidth and a scanning speed of 200 nm/min. Difference spectra were produced by the subtraction of oxidized from reduced spectra, and their amplitudes were normalized for the total membrane protein and for the relative level of wild-type cytochrome expression in the corresponding batch of *Sf9* cells.

The difference spectra from control *Sf9* cells not infected with baculovirus or expressing an unrelated, heme-free protein, XylE, and grown with or without supplementation with ALA and heme lacked significant optical absorbance (traces 5−8 in Figure 5B), showing that the host cell membranes themselves had a negligible level of *b*-type cytochrome.

Reaction of Membranous PAL Mutants of Cyt b_{561} with Ascorbic Acid. Purified wild-type cyt b_{561} was reduced almost fully by ascorbate, the physiological reductant (Figure 3), whereas its membranous counterpart was only ~70% reduced (Figure 6); this difference presumably reflects either changes in the redox potentials of cytochrome or decreased access to the reductant because of membrane components.

The membranous PAL mutants were much less reactive with ascorbate than the wild-type cytochrome. The addition

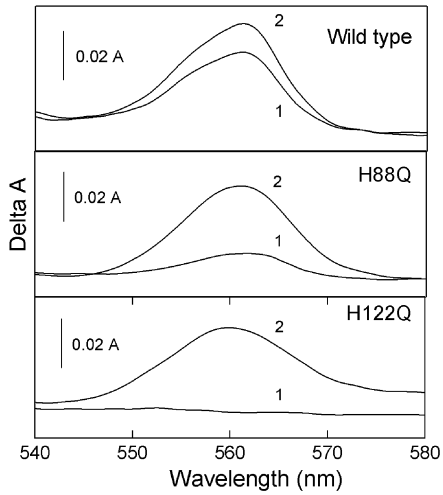

FIGURE 6: Difference optical spectra of *Sf9* cell membranes containing recombinant wild-type cyt b_{561} or two PAL mutants after the reaction with ascorbate (1) and dithionite (2). Membrane suspensions in 60 mM Tris at pH 7.4 containing 20% glycerol were reacted first with 40 mM ascorbate and subsequently with a few grains of dithionite. Absolute absorption spectra were collected for oxidized and reductant-treated samples at 0.1 nm intervals with a 0.05 nm bandwidth and a scanning speed of 40 nm/min. Reduced minus oxidized difference absorption spectra were calculated and normalized to a protein concentration of 1 mg/mL.

of 40 mM ascorbate reduced the mutants at His161 and His88 to ~30% of the extent achieved with dithionite, as illustrated for H88Q (Figure 6). Similar results were reported by Berczi et al. for His88 and His161 (bovine cytochrome numbering) mutants of murine cyt b_{561} expressed in yeast (*21*). Mutants of His54 and His122 were completely unreactive with ascorbate, as shown in Figure 6 for H122Q. This difference in ascorbate reactivity between the His54/His122 and His88/His161 mutant pairs is further evidence that the optical spectra originate from recombinant cyt b_{561} proteins rather than some endogenous *Sf9* cytochrome. The different effects on the ascorbate reactivity of mutations at the two heme centers perhaps reflects changes in the redox potential of the centers, so that the mutation of the center ligated by His54 and His122 causes a larger decrease in the redox potential than the mutation involving the heme center ligated by His161 and His88.

Effects of PAL Mutations on the EPR Spectrum. EPR spectra of membranous cyt b_{561} with mutated PAL are presented on Figure 7 along with the spectra of wild-type cytochrome and control membranes. In the low-spin area, the familiar wild-type signals with g_z at 3.1 and 3.7 are replaced in the mutants with two new low-spin signals. The first signal has $g_z = 2.96$ and $g_y = 2.26$; the second signal is characterized by $g_z = 2.46$ and $g_y = 2.26$. Similar EPR changes were observed when the targeted PAL histidine was substituted with methionine or tyrosine, which are potential axial ligands (Figure 7A) or with glutamine, which does not ligate heme (Figure 7B). In the broader magnetic field interval (shown in Figure 7C for H88Q), a prominent high-spin signal at $g = 6.0$ and non-heme iron $g = 4.3$ signal are observed. A small signal at $g = 1.90$ is associated with $g_z = 2.46$. It is notable that all PAL mutations in either heme center resulted in the appearance of the same set of heme spectral species. Control membranes from cells expressing no cyt b_{561} (with or without the addition of heme and ALA

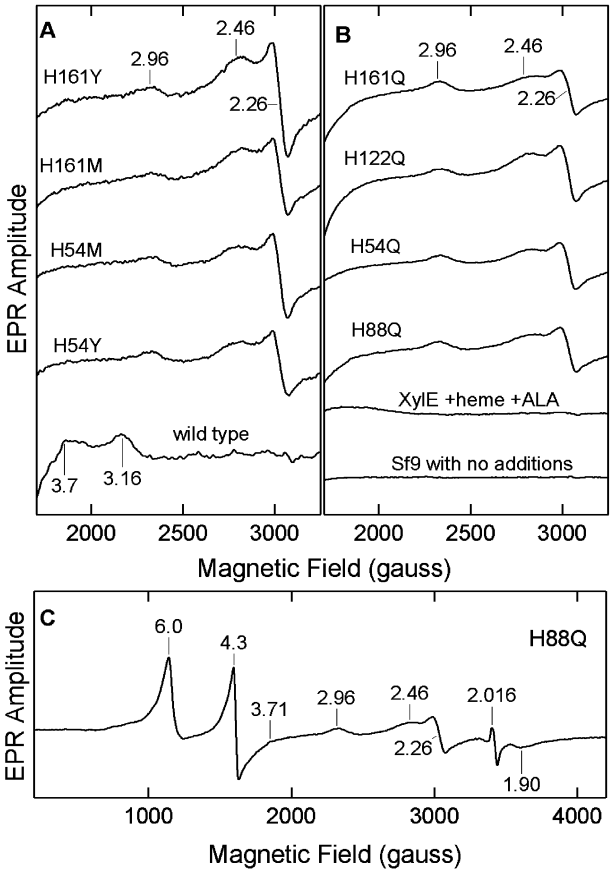

FIGURE 7: EPR spectra of PAL mutants of cyt b_{561} in *Sf9* cell membranes. (A and B) Low-spin region of the EPR spectra of *Sf9* cell membranes containing recombinant wild-type cyt b_{561} and mutants with PAL histidines replaced by methionine or tyrosine (A) or glutamine (B). The spectra of membranes from *Sf9* cells expressing XylE and supplemented with ALA and hemin and membranes from unsupplemented, uninfected *Sf9* cells are presented in B as controls. (C) Wide-scan EPR spectrum of *Sf9* cell membranes containing the H88Q mutant. Membranes were suspended in 20 mM Tris at pH 7.2 containing 20% glycerol. Signal intensities are normalized for the total protein concentration and for the relative level of wild-type cytochrome expression in the corresponding batch of *Sf9* cells. Spectrometer conditions: microwave frequency, 9.60 GHz; microwave power, 1 mW; modulation frequency, 100 kHz; modulation amplitude, 10 G; and temperature, 8 K.

during culture) showed no significant EPR signals (Figure 7B), indicating that the host cell membranes have negligible endogenous EPR-active species.

It is clear from the EPR spectra in Figure 7A that tyrosine substitution at His54 or His161 did not result in the ligation of either heme (*58*); methionine substituted at those positions may have become a ligand (much as reported in ref *57*), producing a complicated situation in which multiple new low-spin signals with slightly different g values can be observed at high microwave power (not shown). These new signals could reflect species with slightly different relative orientations of the remaining histidine and methionine (*59*). In any case, the similarity of the spectra for tyrosine, methionine, and glutamine substitutions at His54 and His122 (panels A and B of Figure 7) indicate that the size and nature of the substituted residue had little effect on the overall outcome; it was the loss of the histidine functionality as the axial ligand that was responsible for the observed effects.

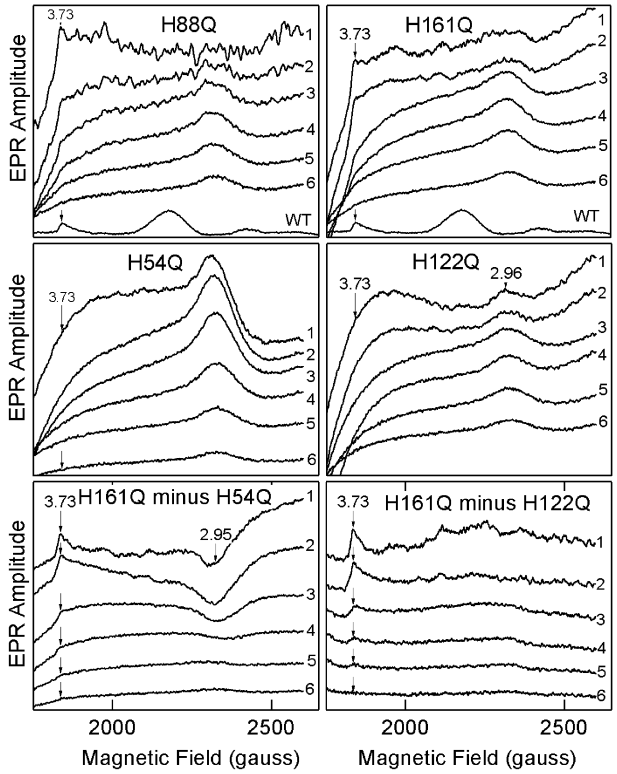

FIGURE 8: Effects of the microwave power on EPR spectra of *Sf9* cell membranes containing glutamine-substituted PAL mutants of cyt b_{561}. The spectra were recorded at 200 (1), 50 (2), 12.8 (3), 3.2 (4), 0.8 (5), or 0.2 (6) mW. Signal intensities were normalized for the total protein concentration in the individual samples. Spectrometer conditions were: microwave frequency, 9.60 GHz; modulation frequency, 100 kHz; modulation amplitude, 10 G; and temperature, 8 K. The two lowest panels represent difference EPR spectra derived from the upper panels as indicated. The spectrum of purified wild-type (WT) cytochrome expressed in *Sf9* cells (collected at 4 mW) is shown in the two upper panels for a comparison.

With one set of PAL mutants in which glutamine was substituted for individual histidines, raising the microwave power from 1 mW (used for the spectra in Figure 7) to higher levels, more favorable for highly axial low-spin (HALS) observation (see the Supporting Information), elicited a signal at $g_z = 3.7$ in the H88Q and H161Q mutants (Figure 8). This indicates that a portion of the low-potential heme center survived the general perturbation of the heme environments caused by these mutations. Importantly, HALS signals were not observed in the H54Q and H122Q mutants (Figure 8). The HALS signals are rather small and under other circumstances might have gone unnoticed because the baselines are far from ideal. To minimize the latter problem, we subtracted the spectrum of the H54Q or H122Q mutant from that of the H161Q mutant at each microwave power. The results (lower two panels in Figure 8) show the appearance of the HALS signal at high powers more convincingly. The presence of the negative peak in the H161Q minus H54Q difference spectrum (lower left panel in Figure 8) reflects the remarkable differences in saturation properties of the signal at $g \sim 2.95$ between the H54Q and H161Q mutants. These EPR results connect the low-potential (HALS) heme center with His54 and His122.

DISCUSSION

EPR Signals of Heme in Wild-Type Cyt b_{561}. The experimental data in this study refute arguments that cyt b_{561} is other than a two heme-containing protein. Burbaev et al. (*41*) found that the $g_z = 3.1$ signal shifts to a lower field with the lowering of the temperature and interpreted this as evidence for a third heme in cyt b_{561}. We reproduced the earlier data in the present experiments by varying the microwave power but also found that similar spectral changes could be demonstrated with cytochrome *c* (Figure 2B). Thus, we believe that the pseudo-heterogeneity of the $g_z = 3.1$ signal is best explained as an artifact that can occur at high power and/or low temperatures.

Wanduragala et al. (*43*) observed that their preparation exhibited only a nominal quantity of the $g_z = 3.7$ signal and raised doubts that this signal originates from an authentic heme center in purified cyt b_{561}. From the power and temperature dependencies of $g_z = 3.1$ and 3.7 signals (see the Supporting Information), one can conclude that the quantity of low-potential heme was substantially underestimated by Wanduragala et al. (*43*) because the EPR conditions that they employed (20 mW and 15 K) are far from optimal for observing the $g_z = 3.7$ species. To address concerns similar to those raised by Wanduragala et al. (*43*) that isolation of cyt b_{561} or even preparation of membranes from CG could cause partial denaturation and the appearance of an additional, non-native EPR signal, we recorded EPR spectra of freshly prepared CG. The resulting EPR spectrum (trace 1 in Figure 1) shows the same EPR signals of cyt b_{561} that are characteristic of the purified and membranous samples of endogenous and recombinant cyt b_{561}, with or without a His tag (*10*, *20*−*22*, *40*−*42*).

Kipp et al. (*44*) discussed the possibility that an EPR signal may be caused by electronic interactions between hemes situated on separate molecules of a cytochrome containing just one heme, thus generating the additional EPR signal, which was, in their view, misinterpreted as the signal of a second heme center in cyt b_{561}. There are several difficulties with this proposal, with the most telling being that the $g_z = 3.7$ resonance should shift to a position approximately midway between the $g_z = 3.7$ and $g_z = 3.1$ signals in partially reduced cytochrome, in which most of the high-potential heme is in the diamagnetic, ferrous state. There is no shift in the $g_z = 3.7$ position in the spectrum of semireduced protein published by Burbaev et al. (*41*), which we now confirm (inset in Figure 1).

Thus, our data provide persuasive evidence for the presence of only two types of hemes in cyt b_{561}. This is consistent with the demonstration that optical changes during reduction are well reproduced using only two components (Figure 4C) and with the published stoichiometry of heme/protein close to 2 in the endogenous (*40*) and recombinant (*20*, *22*) cytochrome. There appears to be no further need to develop models that require other than two hemes per polypeptide of cyt b_{561}.

Low-Spin Heme EPR Signals in PAL Mutants. The mutations of PAL of cyt b_{561} led to the loss of the characteristic low-spin signals from the native high- and low-potential hemes and the appearance of an intense high-spin signal at $g \sim 6$, a low-spin signal with $g_z = 2.96$ and $g_y = 2.26$, and a second low-spin signal with $g_z = 2.46$, $g_y = 2.26$, and $g_x \sim 1.90$ (Figure 7). Similar low-spin signals are known from studies of other cytochromes. An EPR signal with $g_z = 2.96$ was noted as a minor species in some samples of cyt b_{561} (*20*, *21*, *43*, *60*) and in unrelated systems with a mutated cytochrome *b* component (*61*, *62*). This signal has been identified as a "relaxed" conformation of *b*-type cytochrome, in which the strain on heme ligation imposed by the native protein is removed (*63*). The signal with $g_z = 2.46$, $g_y = 2.26$, $g_x \sim 1.90$ resembles those of cyt P-450 (*64*) and P-450 mimics (*65*−*68*). These are hemeproteins, where one of the axial ligands is cysteine and the other is either water, OH^-, histidine, or proline. Cyt b_{561} contains only two cysteines; in the model of Bashtovyy et al. (*3*), these cysteines are located near the M-side heme center. If this model is accurate, Cys57 might replace His54 or Cys125 might replace His122 under the disruption caused by a PAL mutation.[4]

Identification of Axial Ligands for Cyt b_{561} Hemes. In a simple scenario, the absorption spectra of PAL mutants should be sufficient to determine whether particular amino acid residues furnish axial ligands to the cyt b_{561} hemes. With one putative axial ligand eliminated by mutation to glutamine, the affected heme should be converted to a five- or six-coordinated high-spin species, with one axial ligand provided by the unaffected histidine and the second ligand site being either vacant or occupied by water or hydroxide. In this scenario, the second heme of cyt b_{561} is unaffected by mutation and remains low-spin; the resulting absorption spectrum of the PAL mutant exhibits a combination of low- and high-spin features in the Soret and retains roughly half of the intensity in the α-band, where high-spin species have little contribution. The absorption spectra of PAL mutants (parts B and C of Figure 5) indirectly confirm the role of the targeted histidines as axial ligands because, in addition to the typical low-spin peaks, there are some high-spin features in the Soret and in the near-infrared regions that are absent in the wild-type spectrum (Figure 5A). Although the spectra of four different types of control membranes (Figure 5B) convincingly demonstrate that endogenous hemeproteins did not interfere, it was not possible to make a firm estimate of the heme/protein stoichiometry for the PAL mutants in the *Sf9* membranes,[5] and thus a definitive judgment on axial ligation of cyt b_{561} could not be made using optical spectra alone.

Further insights into the consequences of PAL mutations were obtained from the EPR spectra of *Sf9* membranes expressing cyt b_{561} (Figure 7). The initial expectation was that the mutation of either axial ligand to a given heme would perturb only the EPR signal of the affected heme, leaving

[4] The appearance of a P-450-like form of cyt b_{561} under denaturing conditions was noted by Wanduragala et al. [Wanduragala, S., Wimalasena, D. S., Haines, D. C., Kahol, P. K., and Wimalasena, K. (2003) pH-induced alteration and oxidative destruction of heme in purified chromaffin granule cytochrome b_{561}: Implications for the oxidative stress in catecholaminergic neurons, *Biochemistry 42*, 3617−3626], but they did not definitively connect the observed signal with a P-450-like center because they observed a variation in the relative amplitudes of the two components at $g = 2.46$ and 2.26, supposedly the g_z and g_y of the same signal. We suggest that this variation occurs because the g_y of all three minor forms of cyt b_{561} discussed in this paper [the pH-dependent form with $g_z = 2.84$, the species with a "relaxed" conformation ($g_z = 2.96$), and the P-450-like species with $g_z = 2.46$] overlap around $g = 2.26$ and thus make the EPR amplitude at g_y sensitive to the relative amounts of these three minor forms.

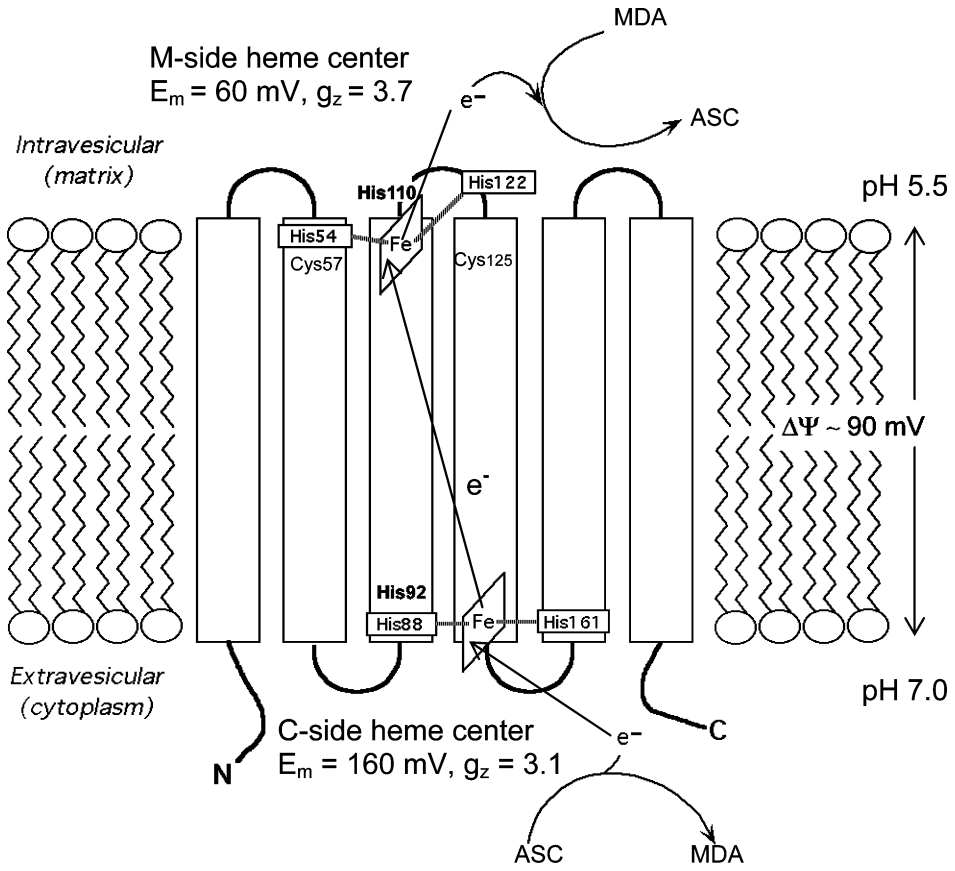

FIGURE 9: Topological model of adrenal cyt b_{561} in the CG membrane. The axial ligation of heme centers is based on proposals by Degli Esposti et al. (*35*) and Okuyama et al. (*49*) and on the results of the present study. The disposition of the low-potential heme on the M side and the high-potential heme on the C side of the membrane is justified in the text. According to the current paradigm, cytoplasmic ascorbate is oxidized to MDA by cyt b_{561}, which shuttles electrons across the membrane and reduces MDA in the matrix. The V_1V_O-type H^+-ATPase (not shown) maintains a transmembrane H^+ electrochemical gradient. Its membrane potential component, $\Delta\psi$, may be important for driving electrons against the gradient of the redox potentials of two hemes of the cytochrome, as discussed in the text. Histidines 122, 54, 161, and 88, marked with boxes, are putative axial ligands to the hemes. ASC, ascorbate and $\Delta\psi$, membrane potential.

the signal of the second heme unchanged. Instead, any substitution at any one of the four PAL histidines resulted in a similar pattern of changes in the EPR spectrum described above. The observation of changes in the EPR spectrum of each of the mutants with affected PALs demonstrates that modification of any of them disrupts the heme environment and thus validates the models of molecular organization of cyt b_{561} introduced by Esposti et al. and Okuyama et al. (*35*, *49*). The global effects of the PAL mutations in cyt b_{561} are reminiscent of results with the cytochrome *b* subunit of quinol:fumarate reductase from *Wolinella succinogenes*, where mutation of any of the four histidines predicted to be axial ligands to the hemes (*69*) resulted in little or no expression of the protein (*70*). Assignment of those histidines as axial ligands was later confirmed by crystallography (*71*).

Mutations of the remaining histidine residues in bovine adrenal cyt b_{561} (His92, His109, and His110) produce recombinant proteins with EPR spectra generally similar to that of the wild-type cytochrome (Liu, W., Rogge, C., Shinkarev, V., Tsai, A.-L, Kamensky, Y., Palmer, G., and Kulmacz, R. J., manuscript in preparation). In murine cyt b_{561}, mutation to alanine of the histidine corresponding to His110 did not affect its absorption spectrum (*21*). Taken together with the results of site-directed mutagenesis of PALs presented here, the accumulated evidence bring the earlier predictions (*35*, *49*) of axial ligation of hemes in cyt b_{561} past the tipping point and leave little doubt that the heme ligation scheme in these models is correct.

The Concept of a Structural Unit Containing Both Heme Centers of Cyt b_{561}. The EPR spectra of mutants in axial ligand residues (Figures 7 and 8) demonstrate that signals from both heme centers in cyt b_{561} are changed dramatically in response to alteration of just one and any one of the four axial ligands to the two hemes. To account for this behavior, we hypothesize that the two hemes and their axial ligands are linked parts of a major structural unit in cyt b_{561} that we term the "kernel". Perturbation of any of the axial ligands leads to structural changes in the whole kernel, including coordination changes at both heme centers.

Three observations illustrate the global response of the kernel to modification of any of its key elements. First, the original high-potential heme signal at $g_z = 3.1$ was not observed in any of the four PAL mutants, suggesting that the high-potential heme center was fully disrupted even though its own axial ligands were not mutated. Second, although the P-450-like signal most likely originates from

[5] Attempts to estimate the quantity of PAL mutant proteins in *Sf9* cell membranes by immunoblotting did not produce satisfactory results because the PAL mutants were refractory to extraction with SDS at room temperature; heating cyt b_{561} in SDS causes aggregation of the protein [Duong, L. T., and Fleming, P. J. (1982) Isolation and properties of cytochrome b_{561} from bovine adrenal chromaffin granules, *J. Biol. Chem. 257*, 8561−8564].

the M-side heme (*3*), with the nearby cysteine residues (Figure 9), the signal with $g_z = 2.46$ appears not only in mutants of His54 and His122 at the M-side center but also in mutants of His88 and His161 at the C-side center (Figure 7). Third, in the framework of the model of Bashtovyy et al. (*3*), it is conceivable that when His88 is mutated it can be replaced by His92. However, the model does not have any histidine residues that could replace His54, His122, and His161 as axial ligands. The signal of a bis-histidine-ligated hemoprotein at $g \sim 2.96$ observed when those histidines were replaced by glutamine (Figure 7B) must originate from the opposite heme center, which was not directly affected by mutation and yet was partially transformed into a "relaxed" conformation (*63*).

The mechanism for transmitting changes in the vicinity of one heme center to the other center is unclear, but because some other cases suggesting "cooperative" behavior involving the heme centers of bis-heme *b*-type cytochromes have been reported (*70*, *72*), this interesting general phenomenon awaits an explanation.

Arrangement of Cyt b_{561} Hemes in the CG Membrane. Earlier topological analyses (*3*, *35*, *49*) have convincingly positioned the His54/His122 pair near the M surface of the CG membrane and the His88/His161 pair near the C surface of the membrane (Figure 9). The question of which heme center is high-potential and which is low-potential has not received much attention apparently because the answer was assumed to be self-evident (*3*, *60*). Physiological electron transfer was presumed to occur down the gradient of ~100 mV between the redox potentials of the two hemes, i.e., from a low-potential heme on the C face of the membrane to a high-potential heme on the M face. However, our EPR data support the opposite topological arrangement of the two heme centers, with the low-potential ($g_z = 3.7$) heme center on the M side ligated by the His54/His122 pair and the high-potential ($g_z = 3.1$) heme center on the C side ligated by the His88/His161 pair (Figure 9). Although the issue of the "sidedness" of the hemes of cyt b_{561} remains to be resolved conclusively, one interesting implication of our topological model (Figure 9) is that physiological transmembrane electron transport, from the cytoplasm to the CG matrix, occurs *against* the ~100 mV gradient of the redox potentials of the two heme centers. We hypothesize that it is the inside-positive membrane potential of up to 90 mV (Figure 9) created by the CG membrane H-ATPase (*73*) that drives electrons "uphill". The role of $\Delta\psi$ as a driving force of electron transport was discussed when cyt b_{561} was thought to contain only one heme (*32*); in the context of our current hypothesis, the suggested role of $\Delta\psi$ becomes even more important. It is noteworthy that, although transmembrane electron transport via adrenal cyt b_{561} has been demonstrated in CG ghosts (*74*) and in reconstituted liposome systems (*31*, *75*−*77*), electron transport was only observed in the non-physiological direction, i.e., from the M side to the C side. We suspect that the membrane potential, absent in these reconstitution experiments, is an important factor modulating the directionality of electron transport.

ACKNOWLEDGMENT

We are indebted to Dr. Vladimir Shinkarev for suggesting the SVD approach and for sharing his experience in its application. We thank Dr. Gary Gerfen for discussion of "passage artifacts" in EPR spectra and Dr. Alexander Konstantinov for critical reading of the manuscript. We are very grateful to Drs. Han Asard and Tibor Pali for sharing the coordinates of their cyt b_{561} computational model, to Dr. Jayashree Soman for help with molecular graphics, and to Ms. Reva Kakkar and Mr. Dazhe Cao for assistance in preparing *Sf9* membrane samples.

SUPPORTING INFORMATION AVAILABLE

Differences in spin-lattice relaxation phenomena for the low- and high-potential hemes of cyt b_{561} and a graph of temperature and power dependencies of the EPR signals of the two hemes. This material is available free of charge via the Internet at http://pubs.asc.org.

REFERENCES

1. Tsubaki, M., Takeuchi, F., and Nakanishi, N. (2005) Cytochrome b_{561} protein family: Expanding roles and versatile transmembrane electron transfer abilities as predicted by a new classification system and protein sequence motif analyses, *Biochim. Biophys. Acta 1753*, 174−190.
2. Verelst, W., and Asard, H. (2003) A phylogenetic study of cytochrome b_{561} proteins, *Genome Biol. 4*, R38.
3. Bashtovyy, D., Berczi, A., Asard, H., and Pali, T. (2003) Structure prediction for the di-heme cytochrome b_{561} protein family, *Protoplasma 221*, 31−40.
4. Verelst, W., and Asard, H. (2004) Analysis of an *Arabidopsis thaliana* protein family, structurally related to cytochromes b_{561} and potentially involved in catecholamine biochemistry in plants, *J. Plant Physiol. 161*, 175−181.
5. Njus, D., and Kelley, P. M. (1993) The secretory-vesicle ascorbate-regenerating system: A chain of concerted H^+/e^--transfer reactions, *Biochim. Biophys. Acta 1144*, 235−248.
6. Klinman, J. P. (2006) The copper−enzyme family of dopamine β-monooxygenase and peptidylglycine α-hydroxylating monooxygenase: Resolving the chemical pathway for substrate hydroxylation, *J. Biol. Chem. 281*, 3013−3016.
7. Ponting, C. P. (2001) Domain homologues of dopamine β-hydroxylase and ferric reductase: Roles for iron methabolism in neurodegenerative disorders? *Hum. Mol. Genet. 10*, 1853−1858.
8. Vargas, J. D., Herpers, B., McKie, A. T., Gledhill, S., McDonnell, J., van den Heuvel, M., Davies, K. E., and Ponting, C. P. (2003) Stromal cell-derived receptor 2 and cytochrome b_{561} are functional ferric reductases, *Biochim. Biophys. Acta 1651*, 116−123.
9. Zhang, D. L., Su, D., Berczi, A., Vargas, A., and Asard, H. (2006) An ascorbate-reducible cytochrome b_{561} is localized in macrophage lysosomes, *Biochim. Biophys. Acta 1760*, 1903−1913.
10. Berczi, A., Su, D., and Asard, H. (2007) An *Arabidopsis* cytochrome b_{561} with trans-membrane ferrireductase capability, *FEBS Lett. 581*, 1505−1508.
11. McKie, A. T., Barrow, D., Latunde-Dada, G. O., Rolfs, A., Sager, G., Mudaly, E., Mudaly, M., Richardson, C., Barlow, D., Bomford, A., Peters, T. J., Raja, K. B., Shirali, S., Hediger, M. A., Farzaneh, F., and Simpson, R. J. (2001) An iron-regulated ferric reductase associated with the absorption of dietary iron, *Science 291*, 1755−1759.
12. Gunshin, H., Starr, C. N., Direnzo, C., Fleming, M. D., Jin, J., Greer, E. L., Sellers, V. M., Galica, S. M., and Andrews, N. C. (2005) Cybrd1 (duodenal cytochrome *b*) is not necessary for dietary iron absorption in mice, *Blood 106*, 2879−2883.
13. Frazer, D. M., Wilkins, S. J., Vulpe, C. D., and Anderson, G. J. (2005) The role of duodenal cytochrome *b* in intestinal iron absorption remains unclear, *Blood 106*, 4413 and author reply 4414.
14. Turi, J. L., Wang, X., McKie, A. T., Nozik-Grayck, E., Mamo, L. B., Crissman, K., Piantadosi, C. A., and Ghio, A. J. (2006) Duodenal cytochrome *b*: A novel ferrireductase in airway epithelial cells, *Am. J. Physiol. Lung Cell Mol. Physiol. 291*, L272−L280.
15. Su, D., May, J. M., Koury, M. J., and Asard, H. (2006) Human erythrocyte membranes contain a cytochrome b_{561} that may be

involved in extracellular ascorbate recycling, *J. Biol. Chem. 281*, 39852−39859.
16. Ji, L., Nishizaki, M., Gao, B., Burbee, D., Kondo, M., Kamibayashi, C., Xu, K., Yen, N., Atkinson, E. N., Fang, B., Lerman, M. I., Roth, J. A., and Minna, J. D. (2002) Expression of several genes in the human chromosome 3p21.3 homozygous deletion region by an adenovirus vector results in tumor suppressor activities in vitro and in vivo, *Cancer Res. 62*, 2715−2720.
17. Ohtani, S., Ueda, K., Jayachandran, G., Xu, K., Minna, J. D., Roth, J., and Ji, L. (2007) Tumor suppressor 101F6 and ascorbate synergistically and selectively inhibit non-small cell lung cancer growth by caspase-independent apoptosis and autophagy. *Cancer Res. 67*, in press.
18. Apps, D. K. (1997) Membrane and soluble proteins of adrenal chromaffin granules, *Semin. Cell Dev. Biol. 8*, 121−131.
19. Kamensky, Y., Kulmacz, R. J., and Palmer, G. (2002) Composition of the heme centers in chromaffin granule cytochrome b_{561}, *Ann. N. Y. Acad. Sci. 971*, 450−453.
20. Liu, W., Kamensky, Y., Kakkar, R., Foley, E., Kulmacz, R. J., and Palmer, G. (2005) Purification and characterization of bovine adrenal cytochrome b_{561} expressed in insect and yeast cell systems, *Protein Expression Purif. 40*, 429−439.
21. Berczi, A., Su, D., Lakshminarasimhan, M., Vargas, A., and Asard, H. (2005) Heterologous expression and site-directed mutagenesis of an ascorbate-reducible cytochrome b_{561}, *Arch. Biochem. Biophys. 443*, 82−92.
22. Liu, W., Rogge, C. E., Kamensky, Y., Tsai, A. L., and Kulmacz, R. J. (2007) Development of a bacterial system for high yield expression of fully functional adrenal cytochrome b_{561}, *Protein Expression Purif.*, in press.
23. Skotland, T., and Ljones, T. (1980) Direct spectrophotometric detection of ascorbate free radical formed by dopamine β-monooxygenase and by ascorbate oxidase, *Biochim. Biophys. Acta 630*, 30−35.
24. Tirrell, J. G., and Westhead, E. W. (1979) The uptake of ascorbic acid and dehydroascorbic acid by chromaffin granules of the adrenal medulla, *Neuroscience 4*, 181−186.
25. Beers, M. F., Carty, S. E., Johnson, R. G., and Scarpa, A. (1982) H^+-ATPase and catecholamine transport in chromaffin granules, *Ann. N. Y. Acad. Sci.* 116−133.
26. Levine, M., Morita, K., and Pollard, H. (1985) Enhancement of norepinephrine biosynthesis by ascorbic acid in cultured bovine chromaffin cells, *J. Biol. Chem. 260*, 12942−12947.
27. Apps, D. K., Pryde, J. G., and Phillips, J. H. (1980) Cytochrome b_{561} is identical with chromomembrin B, a major polypeptide of chromaffin granule membranes, *Neuroscience 5*, 2279−2287.
28. Njus, D., Zallakian, M., and Knoth, J. (1981) The chromaffin granule: Proton-cycling in the slow lane, in *Chemiosmotic Proton Circuits in Biological Membranes* (Skulachev, V. P., and Hinkle, P. C., Eds.) pp 365−374, Addison-Wesley Publishing Company, Inc., Reading, MA.
29. Wakefield, L. M., Cass, A. E., and Radda, G. K. (1986) Electron transfer across the chromaffin granule membrane. Use of EPR to demonstrate reduction of intravesicular ascorbate radical by the extravesicular mitochondrial NADH:ascorbate radical oxidoreductase, *J. Biol. Chem. 261*, 9746−9752.
30. Wakefield, L. M., Cass, A. E., and Radda, G. K. (1986) Functional coupling between enzymes of the chromaffin granule membrane, *J. Biol. Chem. 261*, 9739−9745.
31. Srivastava, M., Duong, L. T., and Fleming, P. J. (1984) Cytochrome b_{561} catalyzes transmembrane electron transfer, *J. Biol. Chem. 259*, 8072−8075.
32. Beers, M. F., Johnson, R. G., and Scarpa, A. (1986) Evidence for an ascorbate shuttle for the transfer of reducing equivalents across chromaffin granule membranes, *J. Biol. Chem. 261*, 2529−2535.
33. Perin, M. S., Fried, V. A., Slaughter, C. A., and Sudhof, T. C. (1988) The structure of cytochrome b_{561}, a secretory vesicle-specific electron transport protein, *EMBO J. 7*, 2697−2703.
34. Tsubaki, M., Kobayashi, K., Ichise, T., Takeuchi, F., and Tagawa, S. (2000) Diethyl pyrocarbonate modification abolishes fast electron accepting ability of cytochrome b_{561} from ascorbate but does not influence electron donation to monodehydroascorbate radical: identification of the modification sites by mass spectrometric analysis, *Biochemistry 39*, 3276−3284.
35. Degli Esposti, M., Kamensky, Y. A., Arutjunjan, A. M., and Konstantinov, A. A. (1989) A model for the molecular organization of cytochrome b_{561} in chromaffin granule membranes, *FEBS Lett. 254*, 74−78.
36. Apps, D. K., Boisclair, M. D., Gavine, F. S., and Pettigrew, G. W. (1984) Unusual redox behaviour of cytochrome b_{561} from bovine chromaffin granule membranes, *Biochim. Biophys. Acta 764*, 8−16.
37. Silsand, T., and Flatmark, T. (1974) Purification of cytochrome b_{561}. An integral heme protein of the adrenal chromaffin granule membrane, *Biochim. Biophys. Acta 395*, 257−266.
38. Duong, L. T., and Fleming, P. J. (1982) Isolation and properties of cytochrome b_{561} from bovine adrenal chromaffin granules, *J. Biol. Chem. 257*, 8561−8564.
39. Wakefield, L. M., Cass, A. E., and Radda, G. K. (1984) Isolation of a membrane protein by chromatofocusing: Cytochrome b_{561} of the adrenal chromaffin granule, *J. Biochem. Biophys. Methods 9*, 331−341.
40. Tsubaki, M., Nakayama, M., Okuyama, E., Ichikawa, Y., and Hori, H. (1997) Existence of two heme B centers in cytochrome b_{561} from bovine adrenal chromaffin vesicles as revealed by a new purification procedure and EPR spectroscopy, *J. Biol. Chem. 272*, 23206−23210.
41. Burbaev, D., Moroz, I. A., Kamenskiy, Y. A., and Konstantinov, A. A. (1991) Several forms of chromaffin granule cytochrome b_{561} revealed by EPR spectroscopy, *FEBS Lett. 283*, 97−99.
42. Kamensky, Y. A., and Palmer, G. (2001) Chromaffin granule membranes contain at least three heme centers: Direct evidence from EPR and absorption spectroscopy, *FEBS Lett. 491*, 119−122.
43. Wanduragala, S., Wimalasena, D. S., Haines, D. C., Kahol, P. K., and Wimalasena, K. (2003) pH-induced alteration and oxidative destruction of heme in purified chromaffin granule cytochrome b_{561}: Implications for the oxidative stress in catecholaminergic neurons, *Biochemistry 42*, 3617−3626.
44. Kipp, B. H., Kelley, P. M., and Njus, D. (2001) Evidence for an essential histidine residue in the ascorbate-binding site of cytochrome b_{561}, *Biochemistry 40*, 3931−3937.
45. Kamensky, Y. A., Arutjunjan, A. M., Ksenzenko, M. Y., Chertkova, E. I., and Konstantinov, A. A. (1990) Axial ligands of haem iron in chromaffin granule cytochrome b_{561}, *Biol. Membr. (USSR) 4*, 667−671.
46. Eaton, W. A., and Hochstrasser, R. M. (1967) Electronic spectrum of single crystals of ferricytochrome *c*, *J. Chem. Phys. 46*, 2533−2539.
47. Myer, Y. P., and Bullock, P. A. (1978) Cytochrome b_{562} from *E. coli*: Conformational, configurational, and spin-state characterization, *Biochemistry 17*, 3723−3729.
48. Arutyunyan, A. M., and Sharonov, Y. A. (1974) Fine structure of the magnetooptical rotatory dispersion curves and the surroundings of heme in ferrocytochrome *c* and its model compounds, *Mol. Biol. 7*, 478−484.
49. Okuyama, E., Yamamoto, R., Ichikawa, Y., and Tsubaki, M. (1998) Structural basis for the electron transfer across the chromaffin vesicle membranes catalyzed by cytochrome b_{561}: Analyses of cDNA nucleotide sequences and visible absorption spectra, *Biochim. Biophys. Acta 1383*, 269−278.
50. Palmer, G. (2000) Electron paramagnetic resonance of metalloproteins, in *Physical Methods in Bioinorganic Chemistry* (Que, L., Ed.) pp 121−186, University Science Books, Sausalito, CA.
51. Rogge, C. E., Liu, W., Wu, G., Wang, L. H., Kulmacz, R. J., and Tsai, A. L. (2004) Identification of Tyr504 as an alternative tyrosyl radical site in human prostaglandin H synthase-2, *Biochemistry 43*, 1560−1568.
52. Berry, E. A., and Trumpower, B. L. (1987) Simultaneous determination of hemes a, b, and c from pyridine hemochrome spectra, *Anal. Biochem. 161*, 1−15.
53. Falk, J. (1964) *Porphyrins and Metalloporphyrins*, p 240, Elsevier, Amsterdam.
54. Carson, M. (1997) Ribbons, *Methods Enzymol. 277*, 493−505.
55. Mailer, C., and Taylor, C. P. (1973) Rapid adiabatic passage EPR of ferricytochrome *c*: Signal enhancement and determination of the spin-lattice relaxation time, *Biochim. Biophys. Acta 322*, 195−203.
56. Takeuchi, F., Kobayashi, K., Tagawa, S., and Tsubaki, M. (2001) Ascorbate inhibits the carbethoxylation of two histidyl and one tyrosyl residues indispensable for the transmembrane electron transfer reaction of cytochrome b_{561}, *Biochemistry 40*, 4067−4076.
57. Matsson, M., Tolstoy, D., Aasa, R., and Hederstedt, L. (2000) The distal heme center in *Bacillus subtilis* succinate:quinone reductase is crucial for electron transfer to menaquinone, *Biochemistry 39*, 8617−8624.

58. Tsai, A. L., Kulmacz, R. J., Wang, J. S., Wang, Y., van Wart, H. E., and Palmer, G. (1993) Heme coordination of prostaglandin H synthase, *J. Biol. Chem. 268*, 8554−8563.
59. Brautigan, D. L., Feinberg, B. A., Hoffman, B. M., Margoliash, E., Peisach, J., and Blumberg, W. E. (1977) Multiple low spin forms of the cytochrome *c* ferrihemochrome. EPR spectra of various eukaryotic and prokaryotic cytochromes *c*, *J. Biol. Chem. 252*, 574−582.
60. Takeuchi, F., Hori, H., and Tsubaki, M. (2005) Selective perturbation of the intravesicular heme center of cytochrome b_{561} by cysteinyl modification with 4,4′-dithiodipyridine, *J. Biochem. (Tokyo) 138*, 751−562.
61. Magalon, A., Lemesle-Meunier, D., Rothery, R. A., Frixon, C., Weiner, J. H., and Blasco, F. (1997) Heme axial ligation by the highly conserved His residues in helix II of cytochrome *b* (*Nar*I) of *Escherichia coli* nitrate reductase A, *J. Biol. Chem. 272*, 25652−25658.
62. Crouse, B. R., Yu, C. A., Yu, L., and Johnson, M. K. (1995) Spectroscopic identification of the axial ligands of cytochrome b_{560} in bovine heart succinate−ubiquinone reductase, *FEBS Lett. 367*, 1−4.
63. Salerno, J. C., and Leigh, J. S. (1984) Crystal field of atypical low-spin ferriheme complexes, *J. Am. Chem. Soc. 106*, 2156−2159.
64. Tsai, R., Yu, C. A., Gunsalus, I. C., Peisach, J., Blumberg, W., Orme-Johnson, W. H., and Beinert, H. (1970) Spin-state changes in cytochrome P-450cam on binding of specific substrates, *Proc. Natl. Acad. Sci. U.S.A. 66*, 1157−1163.
65. Hildebrand, D. P., Ferrer, J. C., Tang, H. L., Smith, M., and Mauk, A. G. (1995) Trans effects on cysteine ligation in the proximal His93Cys variant of horse heart myoglobin, *Biochemistry 34*, 11598−11605.
66. Sigman, J. A., Pond, A. E., Dawson, J. H., and Lu, Y. (1999) Engineering cytochrome *c* peroxidase into cytochrome P450: A proximal effect on heme−thiolate ligation, *Biochemistry 38*, 11122−11129.
67. Smulevich, G., Bjerrum, M. J., Gray, H. B., and Spiro, T. G. (1994) Resonance Raman spectra and the active site structure of semisynthetic Met80Cys horse heart cytochrome *c*, *Inorg. Chem. 33*, 4629−4634.
68. Lanzilotta, W. N., Schuller, D. J., Thorsteinsson, M. V., Kerby, R. L., Roberts, G. P., and Poulos, T. L. (2000) Structure of the CO sensing transcription activator CooA, *Nat. Struct. Biol. 7*, 876−880.
69. Kortner, C., Lauterbach, F., Tripier, D., Unden, G., and Kroger, A. (1990) *Wolinella succinogenes* fumarate reductase contains a dihaem cytochrome *b*, *Mol. Microbiol. 4*, 855−860.
70. Simon, J., Gross, R., Ringel, M., Schmidt, E., and Kroger, A. (1998) Deletion and site-directed mutagenesis of the *Wolinella succinogenes* fumarate reductase operon, *Eur. J. Biochem. 251*, 418−426.
71. Lancaster, C. R., and Kroger, A. (2000) Succinate:quinone oxidoreductases: New insights from X-ray crystal structures, *Biochim. Biophys. Acta 1459*, 422−431.
72. Finegold, A. A., Shatwell, K. P., Segal, A. W., Klausner, R. D., and Dancis, A. (1996) Intramembrane bis-heme motif for transmembrane electron transport conserved in a yeast iron reductase and the human NADPH oxidase, *J. Biol. Chem. 271*, 31021−31024.
73. Johnson, R. G., Carty, S. E., and Scarpa, A. (1981) Proton:substrate stoichiometries during active transport of biogenic amines in chromaffin ghosts, *J. Biol. Chem. 256*, 5773−5780.
74. Njus, D., Knoth, J., Cook, C., and Kelley, P. M. (1983) Electron transfer across the chromaffin granule membrane, *J. Biol. Chem. 258*, 27−30.
75. Russell, J. T., Levine, M., and Njus, D. (1985) Electron transfer across posterior pituitary neurosecretory vesicle membranes, *J Biol. Chem. 260*, 226−231.
76. Kent, U. M., and Fleming, P. J. (1987) Purified cytochrome b_{561} catalyzes transmembrane electron transfer for dopamine β-hydroxylase and peptidyl glycine α-amidating monooxygenase activities in reconstituted systems, *J. Biol. Chem. 262*, 8174−8178.
77. Seike, Y., Takeuchi, F., and Tsubaki, M. (2003) Reversely-oriented cytochrome b_{561} in reconstituted vesicles catalyzes transmembrane electron transfer and supports extravesicular dopamine β-hydroxylase activity, *J. Biochem. (Tokyo) 134*, 859−867.

BI700054G